





Обзор ArXiv/astro-ph, 23-27 сентября 2024

От Сильченко О.К.

ArXiv: 2409.15909

The emergence of galactic thin and thick discs across cosmic history

Takafumi Tsukui,^{1,2*} Emily Wisnioski,^{1,2} Joss Bland-Hawthorn,^{2,3} Ken Freeman^{1,2}

¹*Research School of Astronomy and Astrophysics, Australian National University, Cotter Road, Weston Creek, ACT 2611, Australia*

²*ARC Centre of Excellence for All Sky Astrophysics in 3 Dimensions (ASTRO 3D), Australia*

³*Sydney Institute for Astronomy, School of Physics, A28, The University of Sydney, NSW 2006, Australia*

Accepted XXX. Received YYY; in original form ZZZ

ABSTRACT

Modern disc galaxies commonly have distinct thin and thick discs that are separable in some combination of their kinematics, radial structure, chemistry and/or age. The formation mechanisms of the two discs and the timing of their onset remain open questions. To address these questions, we select edge-on galaxies from flagship JWST programs and investigate their disc structures in rest-frame, near-infrared bands. For the first time, we identify thick and thin discs at cosmological distances, dating back over 10 Gyr, and investigate their decomposed structural properties. We classify galaxies into those that require two discs (thin and thick discs) and those well fitted by a single disc. Disc radial sizes and vertical heights correlate strongly with total galaxy mass and/or disc mass, independent of cosmic time. The structure of thick discs resembles discs found in single-disc galaxies, suggesting that galaxies form a thick disc first followed by thin disc formation. The transition from single to double discs occurred around 8 Gyr ago in high-mass galaxies ($10^{9.75} - 10^{11} M_{\odot}$), earlier than the transition which occurred 4 Gyr ago in low-mass galaxies ($10^{9.0} - 10^{9.75} M_{\odot}$), indicating sequential formation proceeds in a "downsizing" manner. Toomre Q -regulated disc formation explains the delayed thin disc formation in low-mass galaxies, leading to the observed anti-correlation between the thick-to-thin disc mass ratio and total galaxy mass. Despite the dominant sequential formation, observations suggest that thick discs may continue to build up mass alongside their thin-disc counterparts.

Key words: galaxies: high-redshift; galaxies: kinematics and dynamics; galaxies: structure; galaxies: evolution

Из JWST-архивов (NIRCam):

A parent sample is selected based on the `SEXTRACTOR` (Bertin & Arnouts 1996) source catalogues for the JWST mosaic images and then matched with the 3D HST catalogue (Brammer et al. 2012; Momcheva et al. 2016). The JWST source catalogues are publicly available through DJA, compiled by running `SOURCE EXTRACTOR` on the JWST detection image, which is produced by combining available long wavelength filters (F277W+F356W+F444W; Valentino et al. 2023). We extract galaxy parameters from the 3D HST catalogue including redshift, stellar mass, and star formation rate, while parameters from the DJA catalogues include the axis ratio of the galaxy q . A total of 12, 46, and 53 galaxies have spectroscopic, grism, and photometric redshifts, respectively. Galaxies are selected to be edge-on with an axis ratio $q = a/b < 0.3$, a stellar mass $M_* > 10^{8.5} M_\odot$, and well separated from nearby sources by more than $1.5''$. This results in 213 possible sources.

Matching sources against the existing 3D HST catalogue effectively removes erroneous sources from the `SEXTRACTOR` catalog, including the Point Spread Function (PSF) wing of bright stars and parts of nearby spiral galaxies. Moreover, we visually inspect all galaxies, removing cases where galaxies show spiral features (indication of the disc being slightly face-on), significant curvature, and lopsidedness - potentially due to tidal tails and warping. We use multi-wavelength bands (F090W, F115W, F150W, F200W, F277W, F356W, F444W) for visual inspection. For some galaxies, the shortest band (F090W; $0.9\mu\text{m}$) reveals a straight line dust attenuated feature for edge-on galaxies and spiral features for slightly face-on galaxies, helping us to identify edge-on galaxies and non-edge-on galaxies. After visual inspection, the sample includes 132 galaxies.

For the disc structural analysis, we employ NIRCAM F277W: $2.7\mu\text{m}$, F356W: $3.6\mu\text{m}$, F444W: $4.4\mu\text{m}$ filter images for galaxies with redshift $z < 0.46$, $0.46 < z < 0.82$, $0.46 < z < 1.45$, respectively, to maximise overlap with the rest-frame K_s band. For galaxies at $1.45 < z < 2.24$ and $2.24 < z < 3$, we use the F444W band, which corresponds to the rest-frame H and J bands, respectively.



111 галактик

Выборка

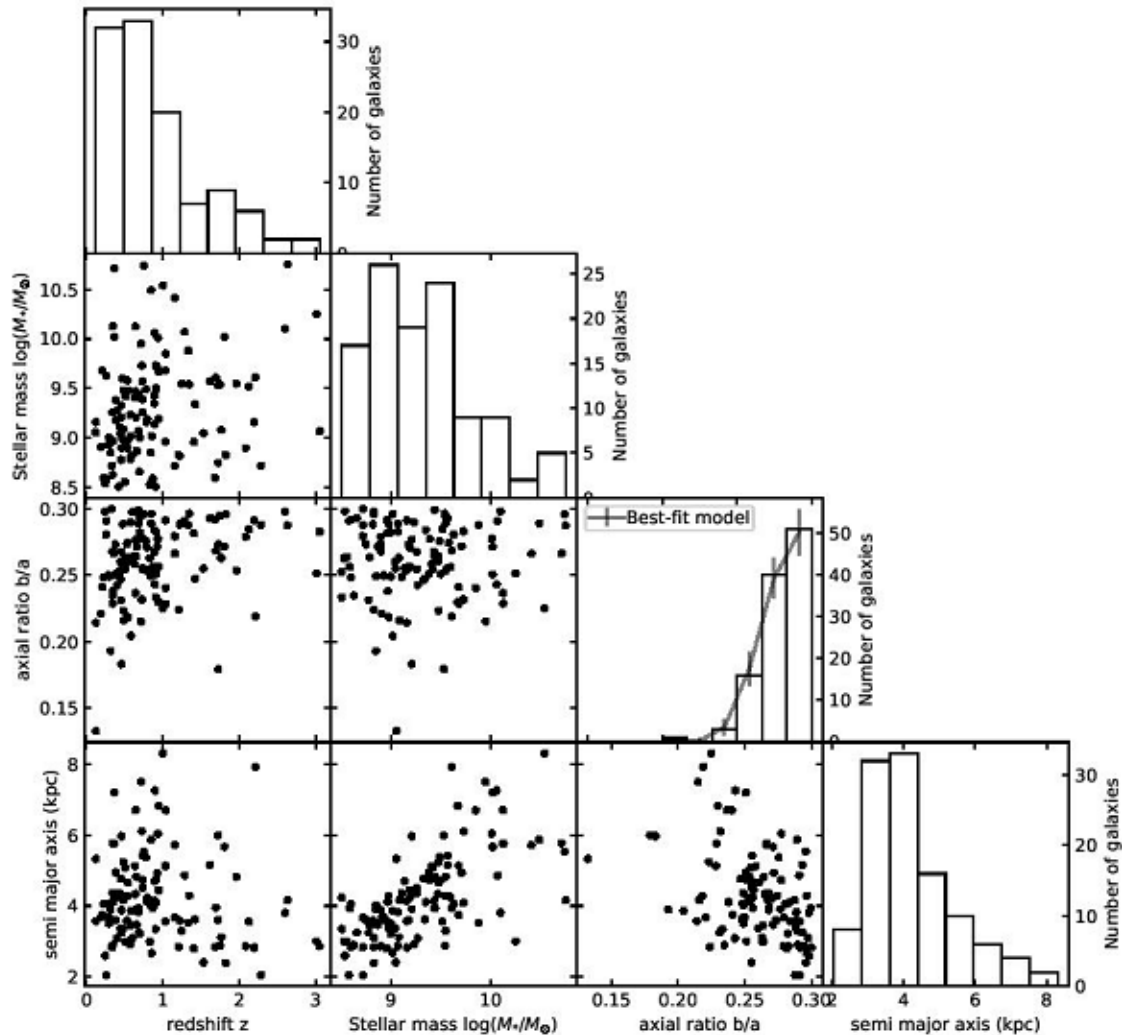


Figure 2. Summary of our 111 edge-on galaxies in redshift z , stellar mass M_* , apparent axial ratio $q = b/a$ and semimajor axis a . The scatter plots illustrate the relationships between each pair of parameters, while the histograms on the diagonal represent the number distribution of each parameter in our sample. The overlaid model line for the axial ratio b/a is the best fit from our population model (Section 2.2).

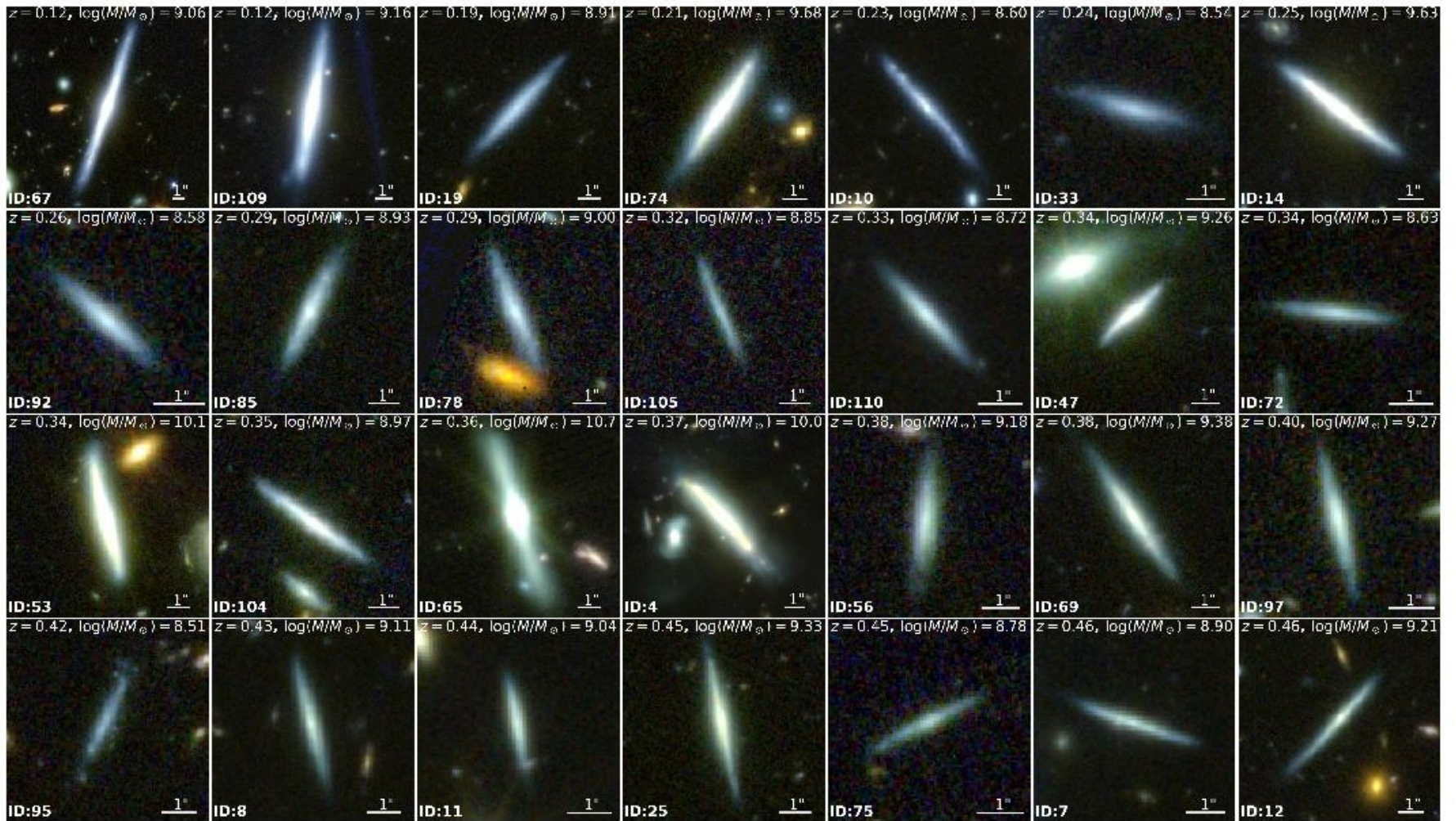
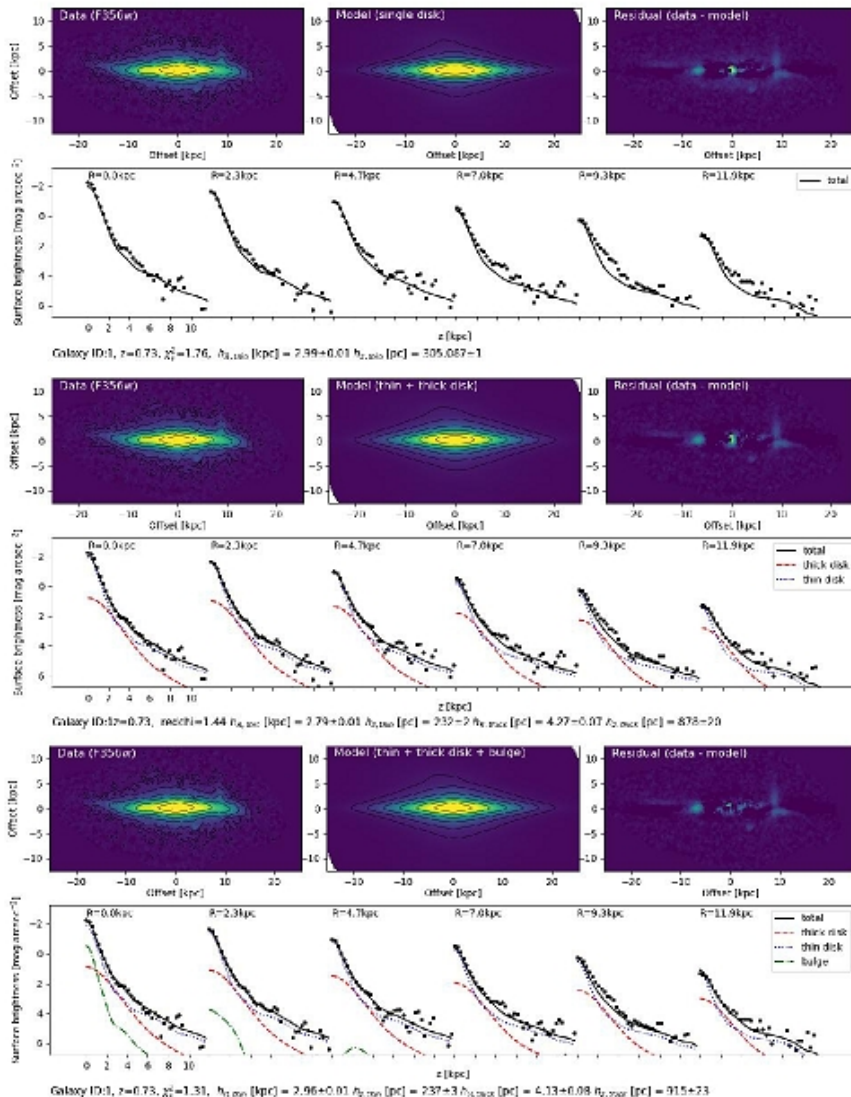


Figure 1. NIRCcam F227W; F356W; F444W colour composite images of a quarter of our sample sorted by increasing redshift. The remainder of the sample is shown Fig. B1, B2 and B3, in Appendix B. The white text on each image indicates the redshift and stellar mass from the 3D HST catalogue as well as the unique ID from this analysis in Table D1. 1" scale is denoted by a white bar in the lower right corner of each cutout.

Подгонка модели (IMFIT):



2.4 3D fitting and model selection

To measure the disc properties (thickness, size, etc) of our edge-on galaxy sample, we use a 3D disc model where the disc luminosity density, $\nu(R, z)$, follows an exponential profile radially and a sech^2 profile vertically. In cylindrical coordinates (R, z) , $\nu(R, z)$ is expressed as:

$$\nu(R, z) = \nu_0 \exp(-R/h_R) \text{sech}^2(z/(2z_0)) \quad (1)$$

where ν_0 is the central luminosity density, and h_R and z_0 represent the disc scale length and height, respectively. The sech^2 profile, a solution for the self-gravitating isothermal sheet (Spitzer 1942), has been widely used to effectively describe and approximate the vertical thickness of galactic discs (van der Kruit 1988; Yoachim & Dalcanton 2008). The generalized function, $\text{sech}^{2/N}$, proposed by (van der Kruit & Searle 1982) describes non-isothermal disc profiles. The model varies from the standard sech^2 profile only near the midplane (van der Kruit & Searle 1982), becoming either peaked or smoothed as N approaches 1 or ∞ , respectively. Despite these differences, all variants of the model asymptotically converge to the exponential profile $\exp(-z/z_0)$ at large distance, z , from the midplane. In the limiting case where $N \rightarrow \infty$, the model matches the exponential profile $\exp(-z/z_0)$ at all radii.

Корреляции с массой:

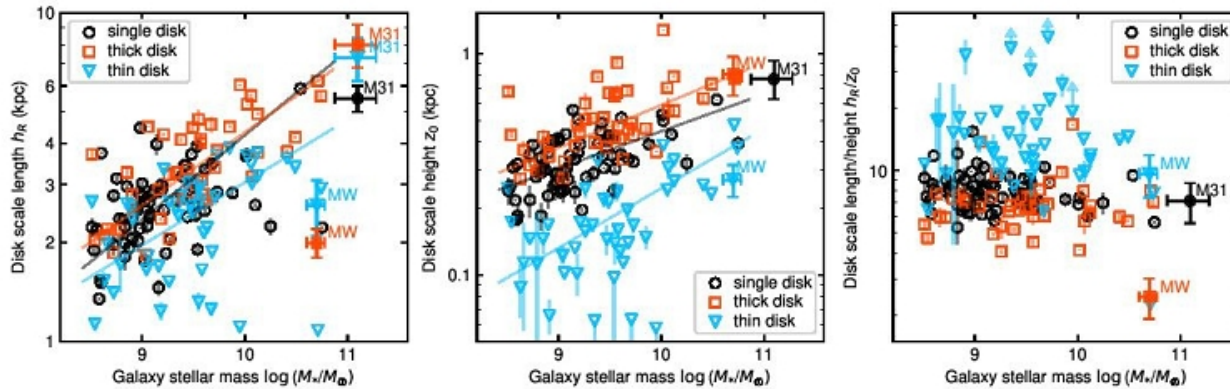


Figure 5. Disc geometrical parameters h_R (left), z_0 (middle) and h_R/z_0 (right) are plotted against galaxy stellar mass M_* . The symbols used are: open black circles for single discs, open blue triangles for thin discs, and open red squares for thick discs in our galaxy sample, covering redshifts from ~ 0.1 to 3. Similar filled symbols represent the thin and thick discs of the Milky Way (Bland-Hawthorn & Gerhard 2016) and M31 (Collins et al. 2011). The measurements assuming a single disc component of M31 by Dalcanton et al. (2023) are also shown.

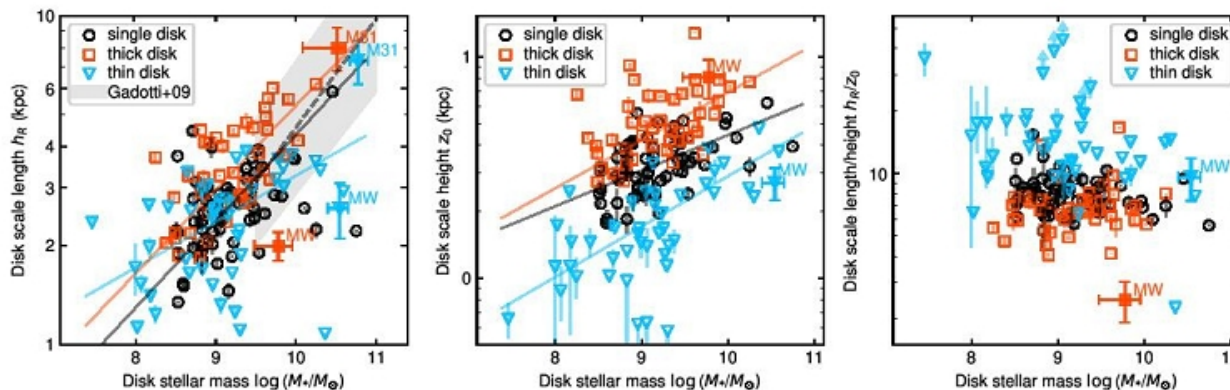


Figure 6. Same symbols as used in Fig. 5, but plotted against the stellar mass of each component rather than the galaxy's total stellar mass. In the left panel showing disc scale length h_R , the scaling relation for the $z = 0$ SDSS sample derived by Gadotti (2009) is shown. We multiply the original relation by 2 to account for suggested systematics in Boardman et al. (2020) due to the galaxy's orientation (see text).

Эволюция с красным смещением (для одиночных дисков)

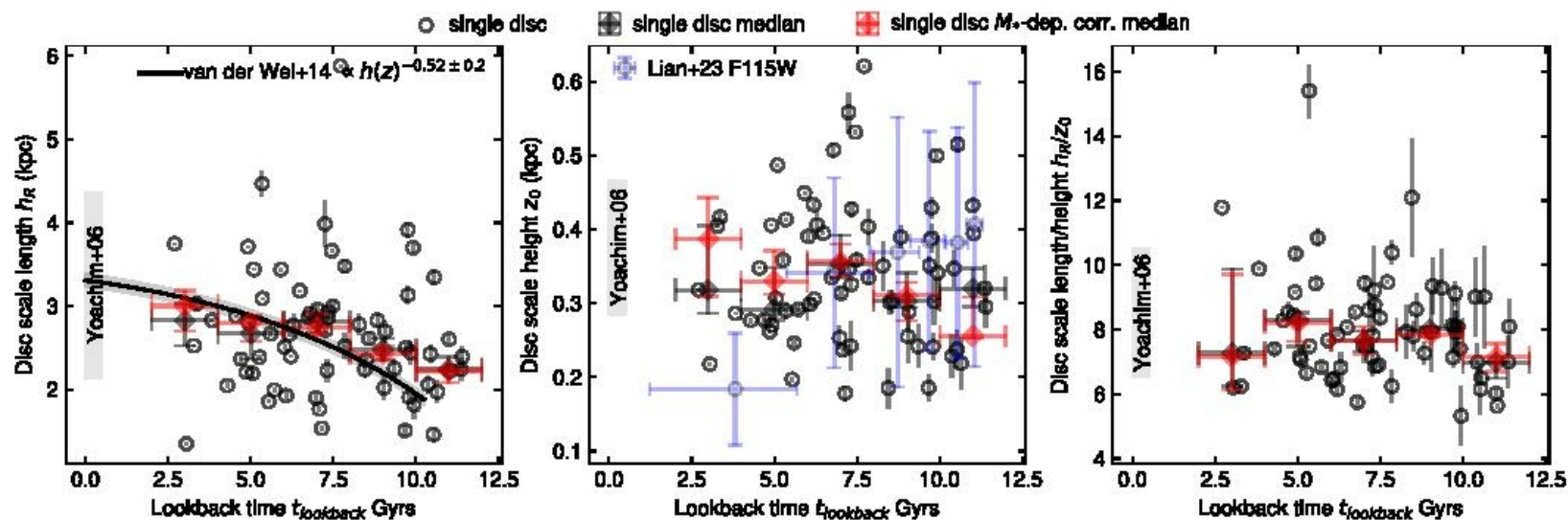


Figure 7. The properties of single discs, h_R (left), z_0 (middle) and h_R/z_0 (right) are plotted against galaxies' lookback time τ_{lookback} . This figure includes only galaxies classified as having a single disc or single disc with a bulge. Black circles show individual measurements with associated 1σ statistical uncertainty (see conservative systematic uncertainty $\sim 20\%$). The large black diamonds indicate the median in each lookback time bin of 2 Gyr widths, with confidence intervals estimated via bootstrap resampling. The red diamonds show the same but linearly corrected for the relation seen in $\log M_* - \log h_R$ and $\log M_* - \log z_0$ to a median $\log(M_* [M_\odot]) = 9.2$ in each bin. The evolutionary trend from van der Wel et al. 2014 for galaxies with stellar mass $\log(M_* [M_\odot]) = 9 - 9.5$ is shown by a black line with an associated 1σ confidence interval for the median. The grey shading near $\tau_{\text{lookback}} \sim 0$ shows the range of values derived by Yoachim & Dalcanton 2006 for $z \sim 0$ sample. The lookback time evolution of z_0 from Lian & Luo 2024 is shown in blue.

Эволюция с красным смещением (для составных дисков)

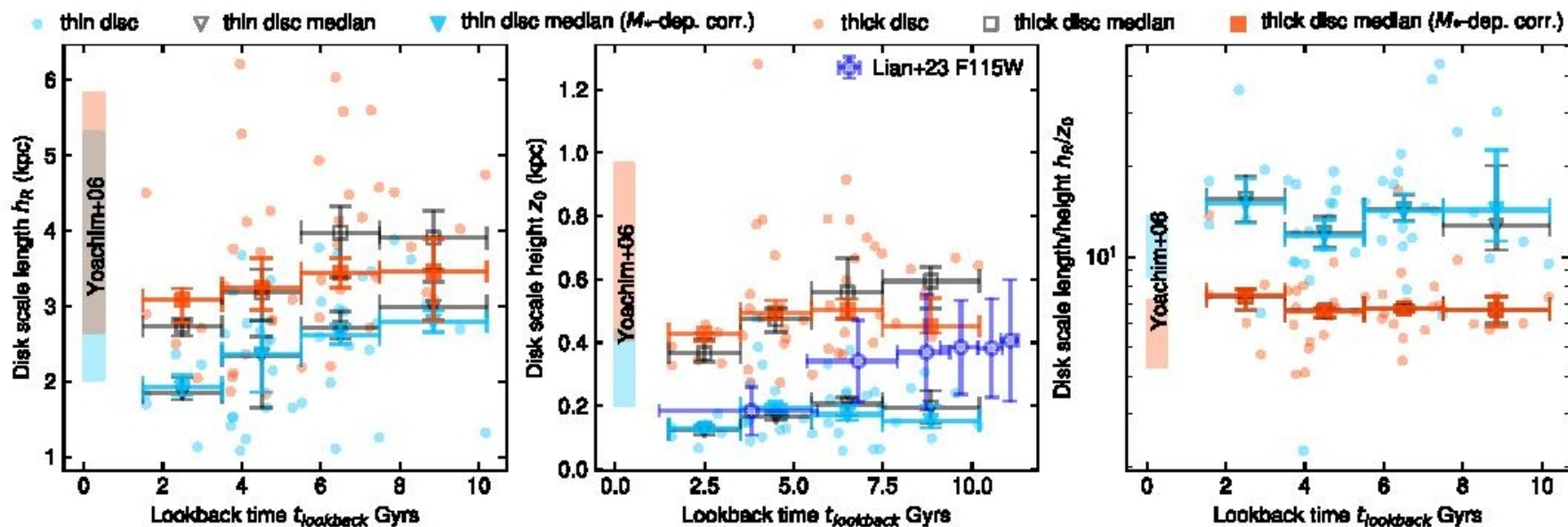


Figure 8. The properties of the thick and thin discs plotted against a galaxy's lookback time. The individual measurements for thin and thick discs are shown in blue and red points, respectively. The black and blue triangles are the median trends of thin disc without and with M_* dependency correction to the stellar mass $\log(M_*/M_\odot) = 9.5$. The black and red squares are the same for thick discs. There is no significant evolution in all properties.

Когда начали формироваться тонкие диски? Downsizing!

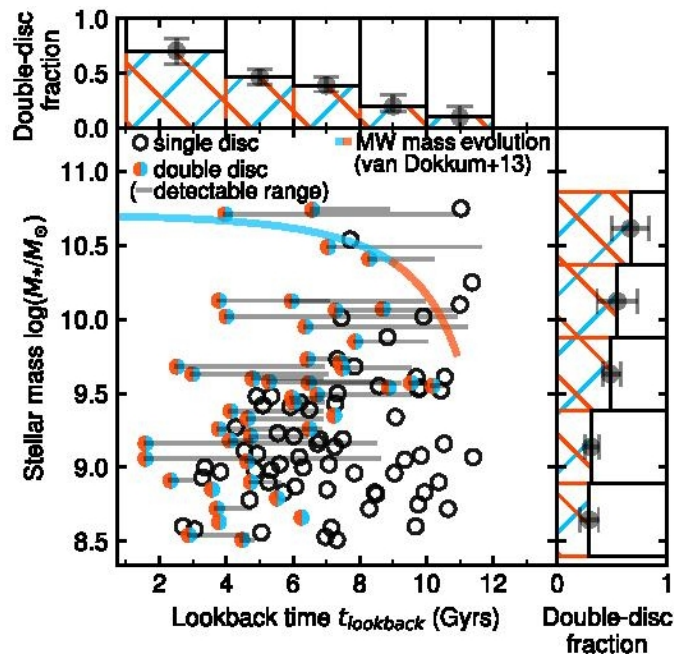


Figure 9. Distribution of two-disc (red-blue points) and single-disc galaxies (black circles) in lookback time and stellar mass. The top and right panels display the fraction of the two disc galaxies as a function of lookback time and stellar mass, with associated 1σ statistical uncertainties⁶. For two-disc galaxies, gray lines indicate the range of lookback times at which galaxies can be identified as having two discs when artificially redshifted. The averaged evolutionary track of Milky Way mass galaxies (van Dokkum et al. 2013) is shown by a blue-red line, where the red part marks the thick disc formation period, and the blue part marks the thin disc formation, with a transition

Почему тонкие диски доминируют в массивных галактиках

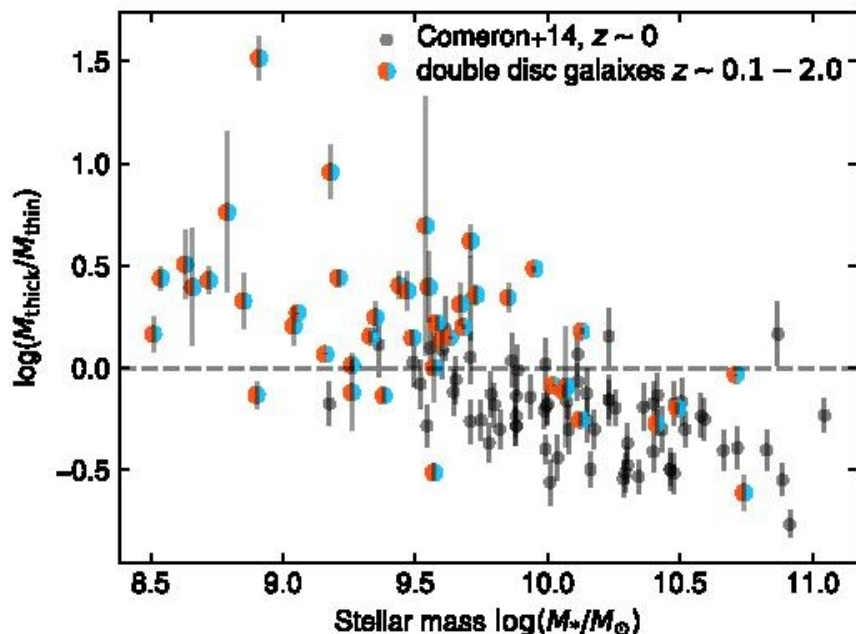


Figure 10. The mass ratio of thick to thin discs plotted against the total stellar mass for two disc galaxies. The red-blue points represent measurements of this work, spanning a redshift range of $z \sim 0.1$ to 2.0. These measurements are taken in bands approximately overlapping rest K_s band at $z < 1.45$ and H band at $1.45 < z < 2.25$. Black points denote measurements from [Comerón et al. 2014](#) for galaxies at $z \approx 0$, obtained using *Spitzer* 3.5 μm and 4.5 μm bands. Error bars indicate the uncertainties associated with each measurements. For visual reference, the dashed line marks the ratio $M_{\text{thick}}/M_{\text{thin}} = 1$.

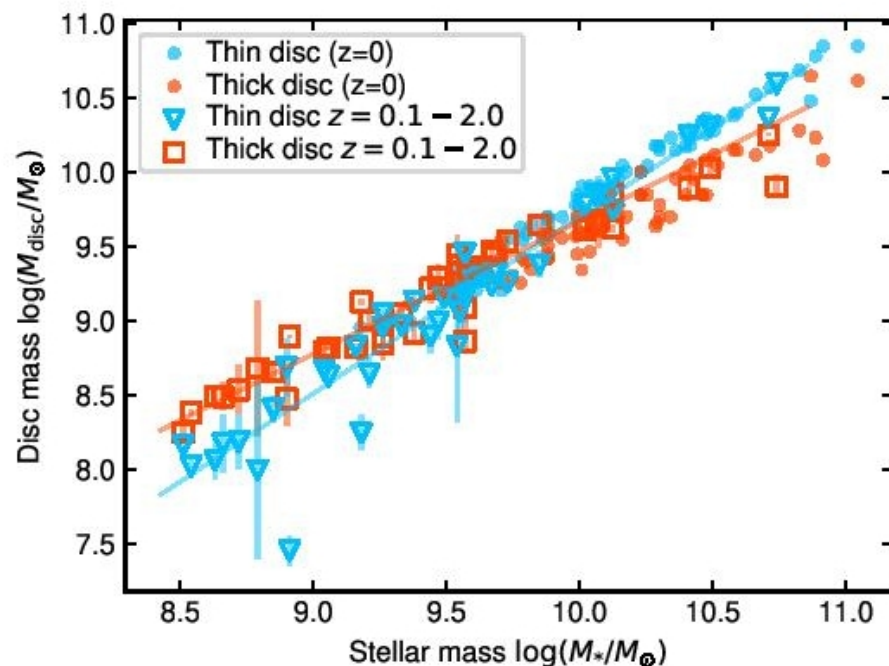


Figure 11. The decomposed thin and thick disc masses of two disc galaxies are plotted against their total stellar masses. Blue triangles represent thin disc measurements, and red squares represent thick disc measurements from this study spanning the redshift range of 0.1 to 2. For comparison, blue and red points indicate thin and thick disc measurements at redshift $z \approx 0$ from [Comerón et al. \(2014\)](#), respectively.

Формирование на месте из газа?

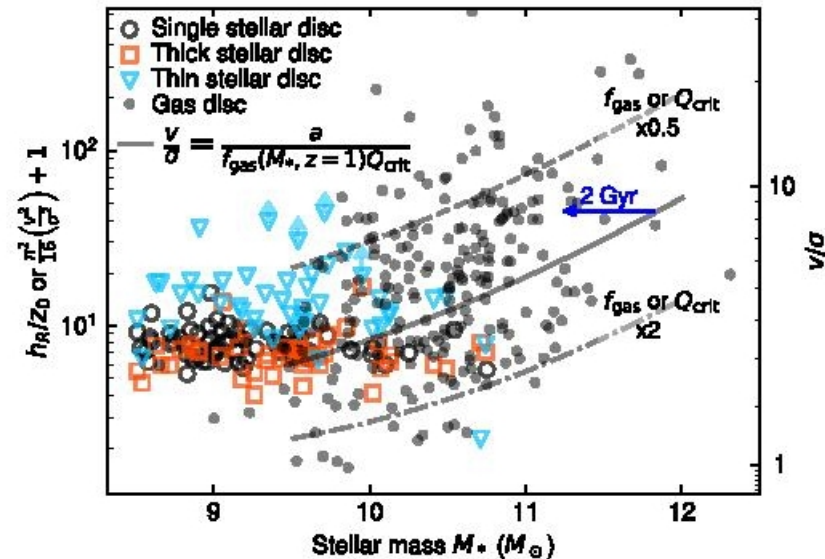


Figure 12. The measured axial ratios for the single disc (black circle), thin discs (blue triangles), and thick discs (red square). The black dots represent the v/σ values for gas discs (Übler et al. 2019, and others⁸), or the expected axial ratios for stellar discs that form from the gas discs in the simplified scenario where the gas disc is entirely converted into a stellar disc while conserving v/σ . The black line indicates the predicted curve for a Toomre Q -regulated gas disc, with $Q_{\text{crit}} = 1$ and $f_{\text{gas}}(M_*)$ for a main-sequence galaxy at $z = 1$ (Tacconi et al. 2020). A 2 Gyr time evolution is illustrated by the blue arrow, which horizontally shifts the curve to the left, allowing more low-mass galaxies to enter the thin-disc formation regime. Variations in the predicted curve, resulting from doubling or halving Q_{crit} , f_{gas} , or the product $Q_{\text{crit}}f_{\text{gas}}$, are shown by dashed and dash-dotted lines.

Динамическая эволюция?

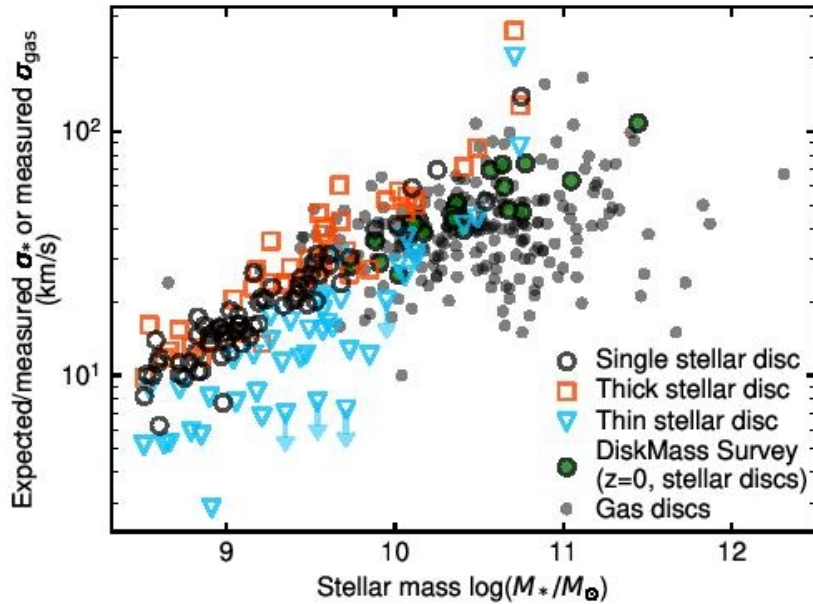


Figure 13. Expected stellar velocity dispersion from vertical equilibrium for single, thin and thick discs, with black circles, blue triangles, and red squares, respectively. Green circles indicate stellar velocity dispersion measurements from the DiskMass survey for face-on galaxies at $z = 0$ (Martinsson et al. 2013b; Martinsson et al. 2013a). These stellar velocity dispersions are compared with those of gas discs.

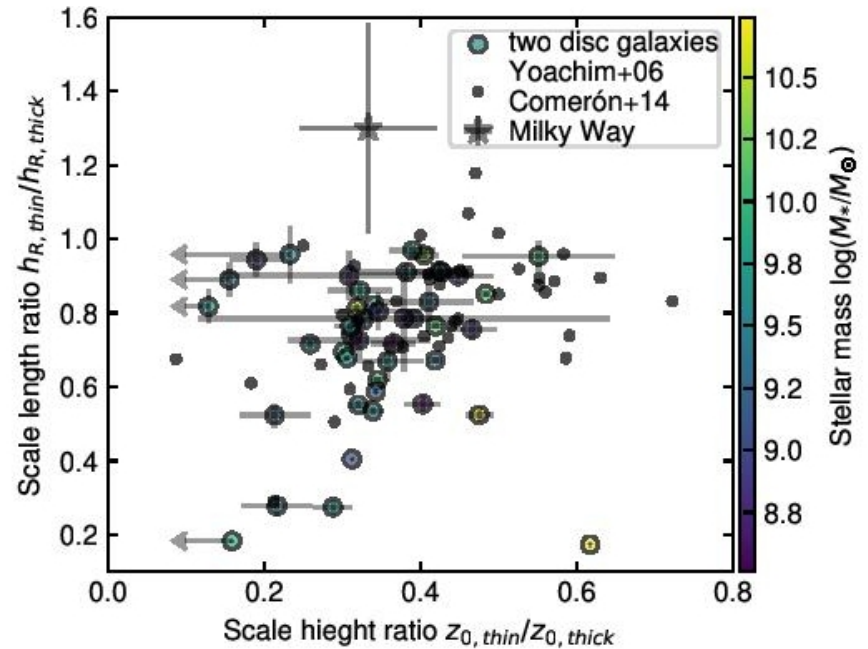


Figure 14. The relative thickness and radial sizes of thin and thick discs in individual two-disc galaxies. The $h_{\text{thin}}/h_{\text{thick}}$ are plotted against $z_{\text{thin}}/z_{\text{thick}}$. The color indicates the mass of the individual galaxies. Galaxies at $z=0$ and Milky Way are overplotted from Yoachim & Dalcanton (2006); Comerón et al. (2018); Bland-Hawthorn & Gerhard (2016).